Supplemental Material

High-resolution imaging of intravascular atherogenic inflammation in live mice

Raphael Chèvre PhD, Jose María González-Granado PhD*, Remco T.A. Megens PhD*, Vinatha Sreeramkumar PhD, Carlos Silvestre-Roig PhD, Pedro Molina-Sánchez BS, Christian Weber MD, Oliver Soehnlein MD PhD, Andrés Hidalgo PhD** and Vicente Andrés PhD**

Online Methods

Mice. Mafia:*ApoE*$^{-/-}$ mice were generated by crossing ApoE$^{-/-}$(Charles River, Lyon, France) with Mafia mice, which express GFP under the control of the *c-fms* promoter.[1] Alternatively, *Lysm*$^{egfp/egfp}$*ApoE*$^{-/-}$ mice[2] were used to visualize myeloid cells. All mice were in the C57BL/6J background and were housed in a pathogen-free barrier facility. For diet-induced atherosclerotic studies, 6 to 8 week-old male mice were fed an atherogenic high-fat diet (HFD: 10.8% total fat, 0.75% cholesterol, S8492-E010, Ssniff, Germany) for the indicated periods of time. All experimental protocols were approved by the local authorities for animal experimentation.

Surgical preparation and stabilization of the carotid artery. Mice were anesthetized with a mixture of ketamine (Imalgene 1000; Merial, France) and medetomidine (Medeson; Urano, Spain) (50 mg/kg and 0.5 mg/kg, respectively). The neck was shaved, and mice were immobilized in *decubitus* position. The right carotid artery was exposed and carefully dissected from the surrounding tissues as described.[3] In short, sutures were used to maintain the salivary gland and adjacent muscles (omohyoid muscle, mastoid part of the sternocephalic muscle and the sternothyroid muscle) away from the artery (Figure1A), and the right vague nerve was carefully separated from the artery. Throughout the procedure, warm saline was applied to the tissues. A flat metal piece with a beveled edge (back end of a surgical blade) was placed under the vessel, while the other side of the piece was fixed to a lateral holder (Figure 1B). Finally, an image-grade round coverslip (12 mm in diameter) cut in half was placed over the artery≈(0.5 mm diameter) and flexibly fixed to the bottom support using water insoluble modeling clay (Figure1C). Gentle pressing on the coverslip led to a separation of approximately 400±50 µm between both supports, which visually restrained the vertical pulsatile movements without significantly compressing the artery. The stabilized region of the artery was then placed under the water-dipping objective of a multichannel epifluorescence microscope or a two-photon microscope equipped with a resonance scanner (Figure 1D). The humidity and temperature of the tissue were maintained through constant dripping of saline at 37ºC delivered onto the objective through a water-jacketed heating coil (Radnoti, Monrovia, CA).

Whole mount confocal laser scanning microscopy. Carotid arteries from Mafia:ApoE$^{-/-}$ mice fed high fat diet for 6 weeks were recovered and fixed in PFA 2% overnight. Whole arteries were mounted under a coverslip and images were captured using a Leica TCS-SP5

confocal scanning laser unit attached to an inverted epifluorescence microscope (DMI6000B) fitted with an 20X/ 0.75 NA multi-immersion objective. 3D reconstruction of arterial wall and atheroma plaque were performed using IMARIS software (Bitplane, Zurich, Switzerland).

Intravital microscopy systems.

The intravital microscopy system was built by 3i (Intelligent Imaging Innovations, Denver, CO) upon an AXIO Examiner Z.1 work station (Zeiss, Oberkochen, Germany) mounted on a 3-Dimensional Motorized Stage (Sutter Instrument, Novato, CA) for fast control of the focal plane and precise computer-controlled lateral movement between XY positions. The microscope was equipped with a CoolLED pE widefield fluorescence LED light source system (CoolLED Ltd. UK), and a quad pass filter cube was used with a Semrock Di01-R405/488/561/635 dichroic and FF01-446/523/600/677 emitter. We used plan-Apochromat 40x NA1.0 and N-Achroplan 10x NA0.3 water-immersion objectives (Zeiss). Images were captured with CoolSnap HQ^2 camera (Photometrics, Tucson, AZ). The SlideBook software 5.0 (Intelligent Imaging Innovations) was run on a Dell Precision T7500 computer system (Dell Inc., Round Rock, TX) to coordinate image acquisition and for offline data analysis.

In some single-channel experiments we also used a Leica DM6000-FS using an Apo 63x NA 0.9 water-immersion objective, equipped with a DFC350-FX camera and the LAS-AF software for acquisition and image processing.

For multidimensional and multichannel imaging, we used an upright Leica SP5II MP TPLSM (Leica Mannheim, Germany) equipped with resonance scanner, a HCX Apo 20 X NA 1.00 water dipping objective and a pre-chirped, pulsed Ti:Sa laser (MaiTai DeepSee HP, Spectra Physics, USA) tuned to 820 nm for two-photon fluorescence excitation. When needed optical zoom was applied to further enhance spatial resolution. Emitted fluorescent signals were detected by three internal Hybrid detectors (HYD) tuned for the corresponding wavelengths using an acousto-optical beam splitter (HYD1; 390-465 nm for autofluorescence of elastin and second harmonics generation of collagen, HYD2; 500-538 nm for GFP and autofluorescence of elastin, HYD3; 570-612 nm for Tritc-Dextran). Single images (512×512 pixels) were recorded in resonance mode in the xy-plane and subsequently collected at successive depths using a Leica galvo-z-drive at 40 Hz (distance between the xy-planes was 0.6-4 µm) and line averaging (3-4 x). The resulting acquisition rate achieved was 7.5-10 Hz. All single images (of XYZT series) were acquired with the aid of respiration triggering to further reduce the movement artifacts caused by respiration. Dependent on the settings, triggered resonance acquisition resulted in an overall temporal

resolution of 1-3 Hz and a spatial resolution of XY≈ 1.5-2.5 µm, Z≈2.0-5.0 µm. Triggering was performed using a small animal trigger unit (Rapid Biomedical, Würzburg, Germany) as described previously.[4] TPLSM data were processed and analyzed with LAS AF 3.0 (Leica), Imagepro Analyzer 3D (version 7.0, Media Cybernetics, USA), and ImageJ 1.47v. Image processing consisted mainly of merging of successive image series, noise reduction performed by 3D Gaussian filtering (n=1; size 3x3 or 5x5; strength 5-8), and generation of maximum intensity extended depth of field projections and 3D (isosurface) reconstructions.

Antibodies. Fluorescently-conjugated anti-mouse CD4 (clone H129.19), CD8a (clone 53-6.7), CD62L (MEL-14), CD41 (clone MWReg30) were purchased from eBiosciences (San Diego, CA) and CD49b (clone HMa2) was purchased from BD Bioscences Pharmingen (San Diego, CA). The JON/A antibody specific for the active form of mouse αIIbβ3 integrin was from Emfret Analytics (Eibelstadt, Germany). The anti-Ly-6G antibody (clone 1A8; BioXcell, Lebanon, NH) was labeled using Dylight 405 and Dylight 650 Antibody Labeling Kits (ThermoScientific; Rockford, IL) following the manufacturer's instructions. For neutrophils and monocytes depletion, the anti-Ly-6G antibody (clone 1A8; BioXcell) and anti-Ly-6G/C antibody (clone GR-1; BioXcell, Lebanon, NH) were injected intra-peritoneally for two days (50 µg / mouse / day). For controls, we injected rat IgG (rIgG, Sigma).

Intravital imaging and analyses.

Detection of VCAM-1 and rhodamine-labeled cells. For luminal detection of VCAM-1, 40 µL of green- Neutravidin-labeled microspheres (Ex/Em 505 / 515, 1 µm in diameter; Molecular Probes) were coupled to 10 µg of biotinylated-anti CD106 antibody (eBioscience). Following manufacturer instructions, beads and antibodies were incubated for 1 hour at room temperature, washed twice and subsequently intravenously injected in ApoE$^{-/-}$ mice right before imaging. As a control, microspheres conjugated with non-specific rat IgG (Sigma) or microspheres alone were injected and did not bind to the atherosclerotic areas. Luminal cells of the carotid artery were labeled by injecting 50 µg of rhodamine 6G (Sigma). Images were acquired under a using a 10x NA 0.3 objective, with 4 x 4 binning in the FITC and Cy3 channels, using a CoolSnap camera. In some experiments, rhodamine-labeled leukocytes were imaged using a 40x NA 1.0 objective. Single-channel acquisitions were performed at speeds of up to 9 Hz.

Labeling of leukocyte subsets and rolling measurements. Circulating leukocytes were labeled *in vivo* by intravenous injection of phycoerythrin (PE)-conjugated anti-CD4 (0.4 µg/mouse), PE-conjugated anti-CD8 (0.4 µg/mouse) and Dy650-conjugated anti Ly6G (1 µg/mouse) antibodies into mice prepared for imaging as described above. Images were captured using a 40x NA 1.0 objective and the CoolSnap camera with 4 x 4 binning in FITC, Cy3 and Cy5 channels (1.7Hz). The number of rolling cells was determined by counting the number of leukocytes crossing an imaginary line perpendicular to the vessel during at least 30 seconds. Several fields (typically 5) were imaged from the carotid bifurcation, or from the common carotid artery, and each data point represents one field. Although the appearance of plaques in the carotid artery is heterogeneous, for visualization we chose areas prone to plaque development (see Figure 1E-F). Data were normalized to the number of rolling cells per minute. Rolling velocity (in µm/s) was determined by measuring time and distances travelled (for an average of 70 µm) by individual leukocytes using a digital caliper with the Slidebook software, (Intelligent Imaging Innovations), and is shown as µm/s. Five to ten leukocytes were analyzed per field and each data point represents one leukocyte.

Leukocyte polarization and crawling. Mafia:*ApoE*$^{-/-}$ mice were injected with an allophycocyanin (APC)-conjugated anti-CD62L antibody (0.5 µg/mouse). Images were captured using the CoolSnap camera with 2 x 2 binning in the FITC and Cy5 channels at 2.5Hz. For offline analyses of CD62L redistribution, a longitudinal line was defined across the middle axis of selected GFP+ cells and fluorescence intensity in the Cy5/APC channel was measured along the line using the Metamorph software (Molecular Devices, Sunnyvale, CA). To track polarization over time, the CD62L+ area associated to a given cell was measured at various time points and normalized as a percentage of the cell area. For off-line analysis of leukocyte crawling and rolling, 33 cells were tracked in the CD62L/Cy5 channel using the ImageJ software (National Institutes of Health, USA), and directionality, distance and velocity of each cell were calculated using built-in algorithms or plug-ins.

Platelet recruitment. To track platelet behavior, we injected Dy650-conjugated anti Ly6G (1 µg/mouse), PE-conjugated anti αIIbβ3 (JON/A; 1 µg/mouse), PE-conjugated anti CD49b (1.6 µg/mouse) [5] and APC-conjugated anti-CD41 (0.4µg/mouse) antibodies into Mafia:*ApoE*$^{-/-}$ mice right before imaging. Images were captured using the CoolSnap camera with 4 x 4 binning in DAPI, FITC, Cy3 and Cy5 channels at 1Hz, or in FITC and Cy5 channels at 2.5Hz. For quantification of platelet adhesion, fields were divided in three categories: "*Low adhesion"* (absence or very low presence of adherent GFP+ myeloid cells),

"*Myeloid clusters"* (strong presence of singly adherent GFP+ cells and small autofluorescent structures), and "*Lesion shoulder"* (presence of three dimensional GFP+ myeloid structures). Activated platelets were defined as CD41+ JON/A+ events. Images were acquired for 1 to 2 minutes, and adherent CD41+ platelets were counted for each field. For plaque reconstruction, images acquired in various regions of atherosclerotic plaques, were manually assembled into a single image. For neutrophil- and monocyte-depletion experiments, anti-Ly6G and anti-Ly6G/C antibodies were injected intraperitoneally (50 µg/mouse/day) for 2 days before imaging. In control groups, rat IgG (Sigma) or saline were injected with identical results. Results are expressed as a percent of the rIgG group.

Intravital microscopy of the cremaster muscle. Mice were anesthetized as indicated above. The cremaster muscle was carefully exteriorized, opened with cautery, and secured across a Plexiglas platform with sutures. Exposed tissues were continuously superfused with endotoxin-free saline warmed to 37°C, and imaging and analyses were performed as reported.[6]

Four dimensional (4D) imaging of cell recruitment and crawling. Prior to TPLSM imaging, *Lysm*$^{egfp/egfp}$*ApoE*$^{-/-}$ mice with fluorescent myeloid cells on HFD for 4 weeks were administered with 150 kDa TRITC- Dextran (Sigma; 2.5µg/100µl) via a jugular vein catheter for discrimination between luminal space and the vessel wall. Imaging was performed in naturally respirated mice at 37°C (using a climate chamber), HBSS solution (Gibco) was constantly perfused in order to maintain the water column between objective and artery. XYZT-stacks were recorded in the mid-section of the stabilized common carotid artery. Acquisition was controlled for each individual optical frame by respiration triggering. The acquisition rate of 7.5-10Hz was sufficiently fast to enable recording of each individual frame in between respiratory cycles (thereby avoiding motion artifacts).

Quantification of arterial stability. To estimate the Pearson's colocalization coefficient of autofluorescent structures in the vessel wall of non-stabilized and stabilized carotid arteries, we acquired image sequences at 5Hz (5 frames per second; for 10x magnification). One focus plane was used as reference, and Pearson's colocalization coefficient was calculated for each frame of a 10 seconds sequence using the Imaris software (Bitplane, Zurich, Switzerland). Graphs represent variations of Pearson's coefficient in colocalized volume over time.

Blood flow analysis. Fluorescent beads (red fluospheres of 1µm diameter, (Ex/Em): (580/605), Invitrogen) were injected intravenously into mice prepared for imaging of the carotid artery. The velocity of movement of free-flowing beads in diastole was evaluated by off-line analysis. For visualization of flow patterns, images were acquired with exposure times of 50 ms.

Flow cytometry. Blood samples taken from mice at different times of diet were lysed to eliminate red blood cells, and leukocytes were washed twice in PBS and incubated 20 min on ice with Dy650-anti-Ly6G, PE-anti-CD8 and PE-anti-CD4. Cells were washed in PBS and samples analyzed with an LSRFortessa analyzer (BD Bioscience, San Diego, CA). Data were analyzed using the DIVA software (BD Bioscience). Leukocyte subsets were identified as follows: Neutrophils, GFP+ Ly6G+; monocytes, GFP+ Ly6GNEG; and T-lymphocytes, GFPNEG;Ly6GNEG CD4/CD8+.

Statistical analyses. Comparison of rolling cell numbers was performed using one-way ANOVA with Turkey's multiple comparison tests for time course comparisons, or two-way ANOVA with Bonferroni correction for multigroup comparisons. The correlation of rolling numbers and velocities was assessed by linear regression tests with 95% of confidence interval. Platelet adhesion was analyzed using one-way ANOVA and Turkey's multiple comparison test to compare all groups with each other. For flow cytometric experiments, we used two-way ANOVA with Bonferroni correction. The GraphPad Prism 5 software was used for all statistical analyses. P values below 0.05 were deemed significant.

References

1. Burnett SH, Kershen EJ, Zhang J, Zeng L, Straley SC, Kaplan AM, Cohen DA. Conditional macrophage ablation in transgenic mice expressing a Fas-based suicide gene. *J Leukoc Biol.* 2004;75(4):612-623.

2. Rotzius P, Soehnlein O, Kenne E, Lindbom L, Nystrom K, Thams S, Eriksson EE. ApoE(-/-)/lysozyme M(EGFP/EGFP) mice as a versatile model to study monocyte and neutrophil trafficking in atherosclerosis. *Atherosclerosis.* 2009;202(1):111-118.

3. Doring Y, Drechsler M, Wantha S, Kemmerich K, Lievens D, Vijayan S, Gallo RL, Weber C, Soehnlein O. Lack of neutrophil-derived CRAMP reduces atherosclerosis in mice. *Circ Res.* 2012;110(8):1052-1056.

4. Megens RT, Reitsma S, Prinzen L, oude Egbrink MG, Engels W, Leenders PJ, Brunenberg EJ, Reesink KD, Janssen BJ, ter Haar Romeny BM, Slaaf DW, van Zandvoort MA. In vivo high-resolution structural imaging of large arteries in small rodents using two-photon laser scanning microscopy. *J Biomed Opt.* 2010;15(1):011108.

5. Jenne CN, Wong CH, Petri B, Kubes P. The use of spinning-disk confocal microscopy for the intravital analysis of platelet dynamics in response to systemic and local inflammation. *PLoS One.* 2011;6(9):e25109.
6. Chiang EY, Hidalgo A, Chang J, Frenette PS. Imaging receptor microdomains on leukocyte subsets in live mice. *Nat Methods.* 2007;4(3):219-222.

Online Figures

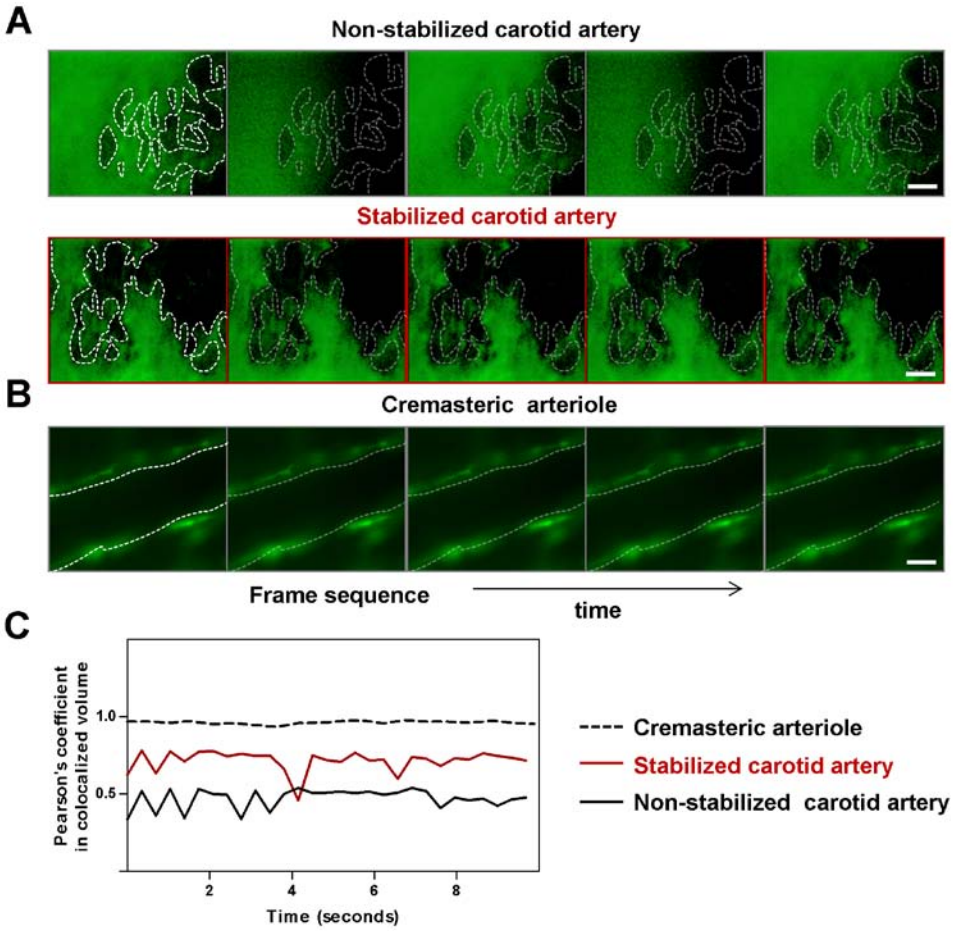

Online Figure I. Stability of the carotid artery.

(**A**) Image sequence of the carotid artery with or without stabilization from a movie captured at 3 Hz. The signal (green) corresponds to autofluorescence of the arterial wall. White dashed lines delimitate reference structures in the initial image, which remain fixed only in the stabilized preparation. Scale bars, 40 µm. (**B**) Image sequence of an arteriole in the stabilized cremaster muscle of a Mafia:ApoE$^{-/-}$ mouse, from a movie captured at 3 Hz. Scale bar, 40µm. (**C**) Graphical representation of Pearson's co-localization coefficient, which has a value of 1 when total colocalization occurs. Correlative images acquired under a 40x objective were aligned with a selected focus plane. Pearson's coefficient of fluorescent vessel wall structures was calculated for each time point.

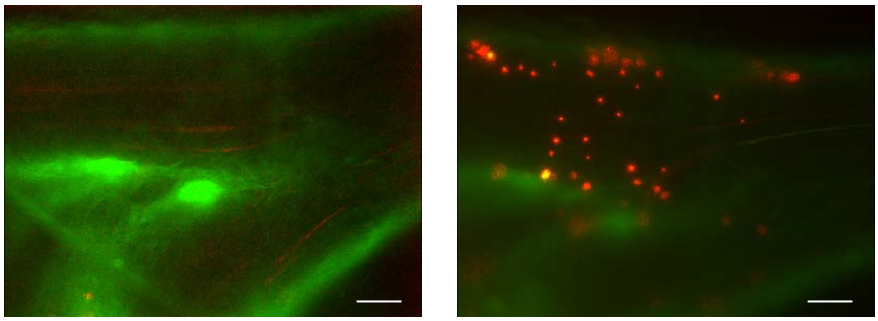

rIgG/microspheres **VCAM-1/microspheres**

Online Figure II. Anti-VCAM-1 coated beads bind specifically to the carotid bifurcation

Fluorescent beads (red) conjugated to control rat IgG (rIgG) do not bind to atherogenic regions of the carotid artery (left panel) in fat-fed ApoE$^{-/-}$ mice, whereas beads conjugated to anti-VCAM-1 antibody accumulate at bifurcation areas (right panel). Scale bar: 200µm.

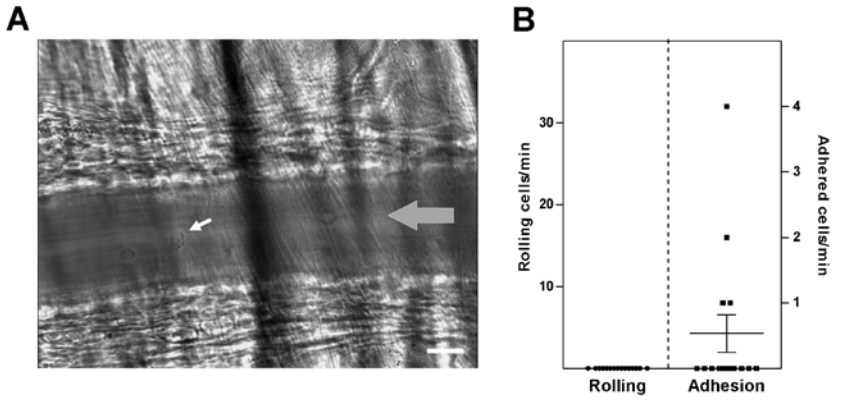

Online Figure III. Absence of leukocyte recruitment in arterioles of the microcirculation during atherogenesis.

The cremaster muscle of ApoE-/- mice fed HFD for 3 weeks was analyzed by intravital microscopy. (**A**) Representative image of an arteriole with a single adherent leukocyte (small arrow). The large arrow shows the direction of flow. Scale bar, 20µm. (**B**) Quantification of the number of rolling and adherent cells in cremasteric arterioles. n=15 arterioles from 3 mice.

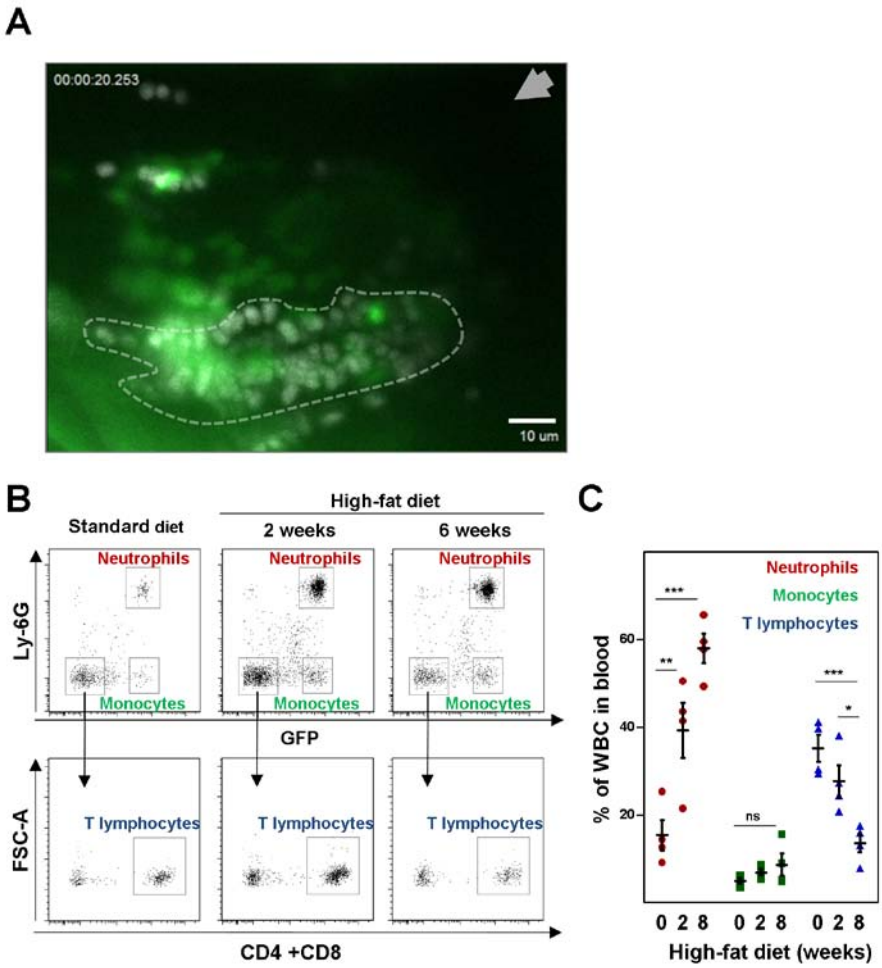

Online Figure IV. Tracking leukocyte subsets in atherosclerotic mice.

(**A**) Representative image showing the tracks left by rolling leukocytes during 20s on the lumen of the carotid bifurcation of a fat-fed Mafia:ApoE$^{-/-}$ mouse. Dashed lines highlight a region of preferential rolling in this experiment. (**B**) Flow cytometry plots of blood leukocytes from Mafia:ApoE$^{-/-}$ mice before and after 2 or 8 weeks on HFD. Leukocytes subsets were labeled with antibodies against Ly6G, CD4 and CD8. (**C**) Frequency of GFP+ Ly6G+ neutrophils, GFP+ Ly6G^{NEG} monocytes and GFP^{NEG} CD4/CD8+ T lymphocytes in the blood of the mice shown in (B). Data represent mean ± s.e.m. from n=4 mice. **P*<0.05, ***P*<0.01, ****P*<0.001; ns, not significant.

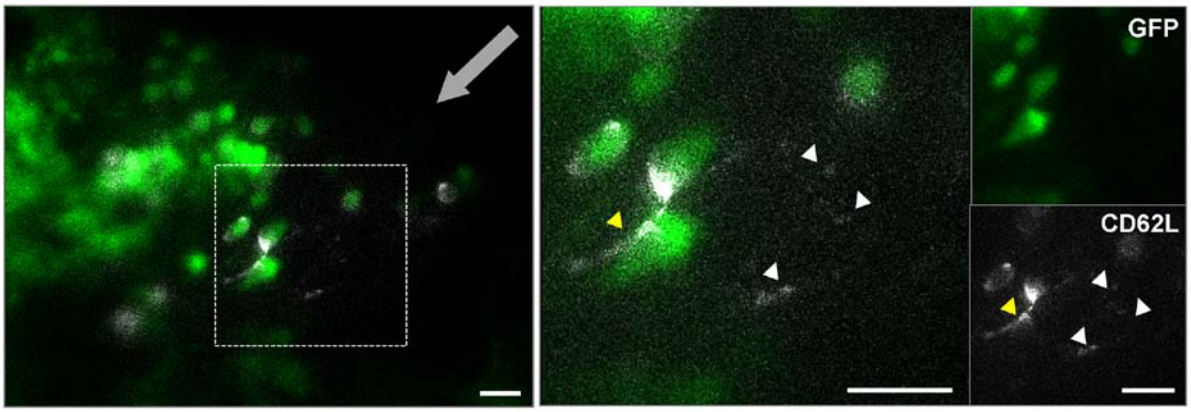

Online Figure V. Visualization of CD62L-immunoreactive membrane fragments.

Mafia:ApoE$^{-/-}$ mice fed for 3 weeks with HFD were injected with a fluorescently-conjugated anti-CD62L antibody. The left micrograph shows polarized GFP+ CD62L+ cells. The enlarged image in the middle shows one polarized GFP+ cell leaving a CD62L+ track (yellow arrowhead), as well as dispersed CD62L+ debris (white arrowheads) on the endothelium. Scale bars, 10 μm.

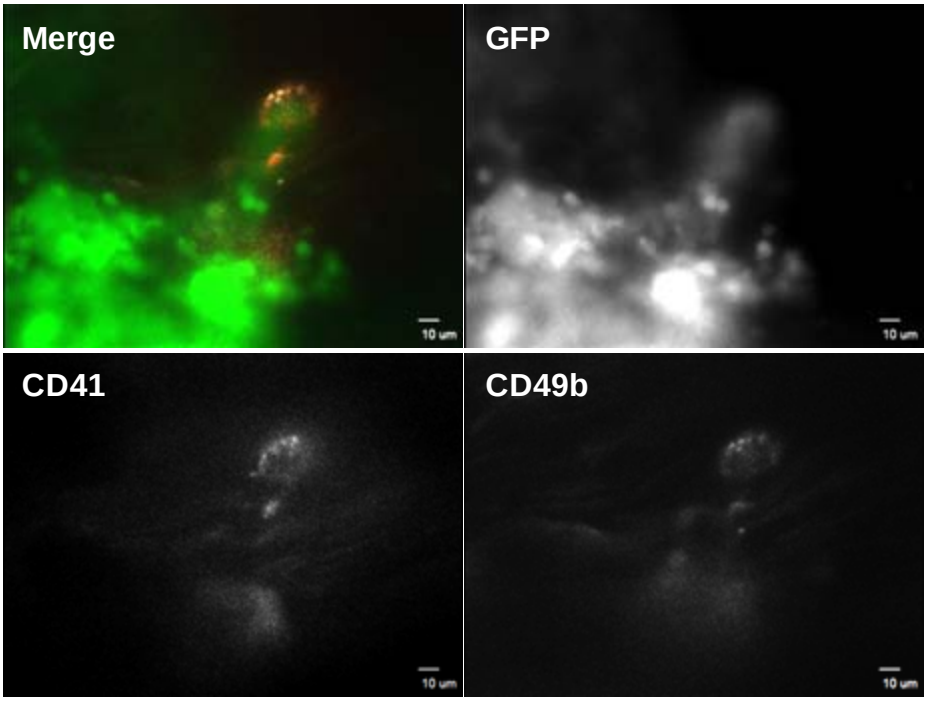

Online Figure VI. CD49b colocalizes with CD41 in platelets.

Mafia:ApoE$^{-/-}$ mice were fed HFD for one month and injected with an APC-conjugated antibody against CD41 and PE-conjugated antibody against CD49b before imaging. Representative images panels show myeloid leukocytes (green) interacting with platelets which are CD41 and CD49b positive (red/yellow respectively). Scale bars, 10μm.

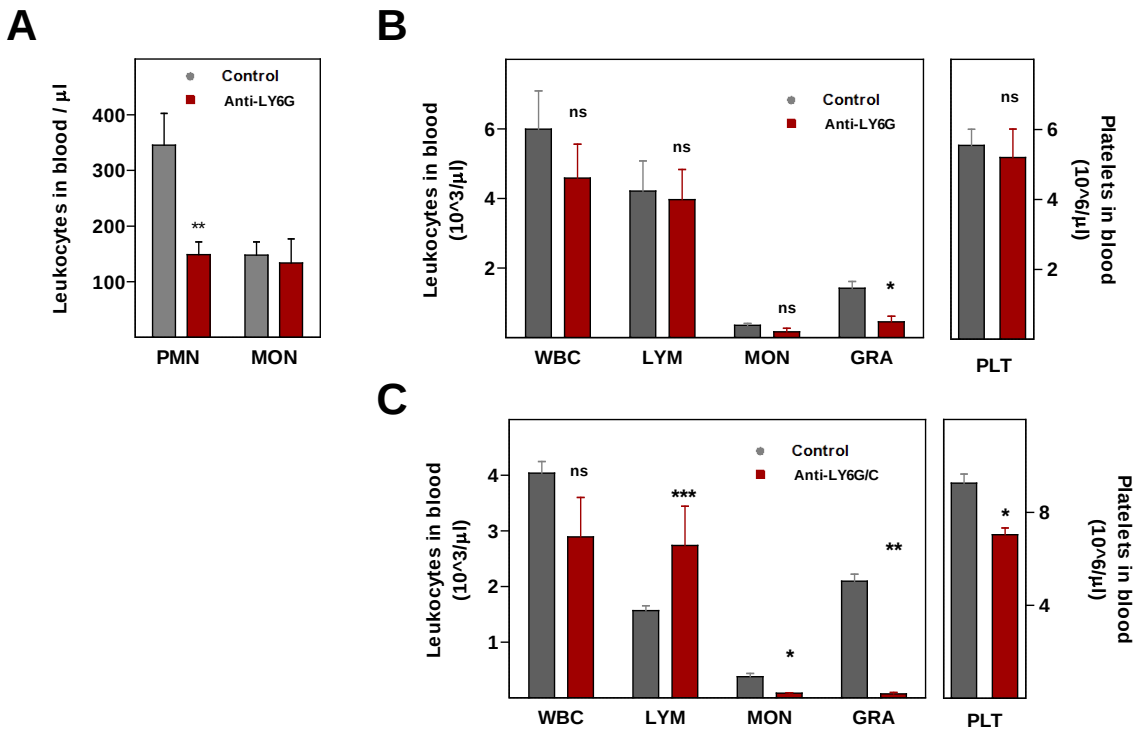

Online Figure VII. Blood populations after αLy6G and αLy6G/C depletion

(**A**) Neutrophil (PMN) depletion with Ly6G (1A8) does not affect monocyte (MON) number. A group of 9 mice was injected with Ly6G antibody (clone 1A8, red bars) of control rIgG (grey bars) (both at 50 µg/day for 2 days, i.p.). (**B, C**) Blood populations after αLy6G and αLy6G/C depletion. Mafia:ApoE$^{-/-}$ mice fed for 1 month with HFD were injected with anti-Ly6G (**B**) or anti-Ly6G/C (**C**) antibodies for two days. Histograms show hematological analysis performed using Abacus Junior (Diatron). Absolute number of total white blood cells (WBC), Lymphocytes (LYM), Monocytes (MON), granulocytes (GRA) and platelets (PLT) are shown. Grey bars show blood counts before depletion, red bars show blood counts after depletion. * p<0.05, ** p<0.01, *** p<0.001

Online Movie Captions

Online Movie I	Real-time imaging of a non-stabilized (left video) and stabilized (right video) carotid artery in ApoE$^{-/-}$ mice. Green signal is autofluorescence. Strong lateral and vertical movements can be appreciated in the left video. After stabilization, vertical movements are markedly reduced and only some lateral movements can be appreciated. Scale bar, 100 µm.
Online Movie II	Free-flowing fluorescent beads (red) on a stabilized carotid artery (green autofluorescence). Red tracks show the flow pattern of the beads, corresponding to their displacement during 50 ms. Movie-rate has been accelerated 3 times. Scale bar, 100 µm.
Online Movie III	GFP Myeloid cells (green) accumulate to form atheroma plaque at the level of the carotid bifurcation in Mafia: ApoE$^{-/-}$ mice fed a high-fat diet for 2 months. Rhodamine 6G (red) was injected to label luminal cells. Movie rate has been accelerated 3 times. Scale bar, 100 µm.
Online Movie IV	High magnification (40X objective) imaging of a non-stabilized (left) and stabilized (right) carotid artery in ApoE$^{-/-}$ mouse fed a high-fat diet for 4 weeks. An anti-CD11b antibody was injected to label luminal myeloid cells (blue) and an anti-CD41 to label platelets (red). Strong lateral and vertical movements can be appreciated in the left video. Vertical movements are strongly reduced and only some lateral movements can be appreciated after stabilization, allowing better imaging of bound leukocytes and platelets. Movie rate has been accelerated 3 times. Scale bar, 10 µm.
Online Movie V	Rhodamine-labeled leukocytes rolling or adhered on the endothelium of a stabilized carotid artery of an ApoE$^{-/-}$ mouse fed a high-fat diet for 4 weeks. Individual endothelial cells can also be visualized. Movie-rate has been accelarated 3 times. Scale bar, 10 µm.
Online Movie VI	GFP-positive myeloid cells rolling, adhered or extravasated in a stabilized carotid artery of a Mafia: ApoE$^{-/-}$ mouse fed high-fat diet for 10 days. Movie-rate has been accelarated 3 times. Scale bar, 10 µm.
Online Movie VII	Polarization and crawling of leukocytes on the atherogenic endothelium of a Mafia: ApoE$^{-/-}$ mouse fed a high-fat diet for 3 weeks. One GFP+ cell arrives to this area, adheres and polarizes to form an CD62L+ uropod (white). Another GFP+ cell with a pre-formed CD62L+ uropod crawls against the flow. Movie-rate has been accelerated 40 times. Scale bar, 10 µm.
Online Movie VIII	CD41-positive platelets (red) are not recruited to areas devoid of GFP+ myleoid leukocytes in the carotid artery of a Mafia: ApoE$^{-/-}$ mouse fed a high-fat diet for 4 weeks. Movie-rate has been accerlated 5 times. Scale bar, 10 µm.

Online Movie IX	Recruitment of CD41+ platelets (red) to lesions containing GFP+ myeloid cell clusters in the carotid artery of a Mafia: ApoE$^{-/-}$ mouse fed a high-fat diet for 4 weeks. Movie shows 2 different fields. Movie-rate has been accelerated 4 and 5 times. Scale bar, 10 µm.
Online Movie X	Four channel imaging of the luminal atheroma. Mafia: ApoE$^{-/-}$ mice were fed a high-fat diet for 4 weeks and injected with different fluorescently-labeled antibodies before imaging. High-speed acquisition allows identification of neutrophils (anti-Ly6G-Dy405, purple); myeloid leukocytes (GFP+, green); activated platelets (JON/A-PE, yellow) and total platelets (CD41, red); Platelets appear bound in regions containing GFP+ cells. Only the larger platelet cluster shows activation (JON/A+). The Movie shows 4 individual channels (from left to right: Ly6G-Dy405, myeloid cells-GFP, JON/A-PE, CD41-APC). The far-right video shows the merged channels. Movie-rate has been accelerated 10 times. Scale bar, 10 µm.
Online Movie XI	Two-photon imaging of the stabilized carotid artery of *Lysm*$^{egfp/egfp}$*ApoE*$^{-/-}$ mice showing GFP+ myeloid cells crawling on the arterial wall at low magnification. Images are presented as 2D extended depth-of-field pictures using maximum intensity projection. Green are myeloid cells, blue shows collagen-derived second harmonic generation in the tunica adventitia, grey represents autofluorescence of the extracelular matrix in the tunica media; and red is 150kDa TRITC-Dextran in the circulating blood, thus demarcating the lumen. Scale bar, 75 µm.
Online Movie XII	Two-photon imaging of the stabilized carotid artery of *Lysm*$^{egfp/egfp}$*ApoE*$^{-/-}$ mice showing GFP+ myeloid cells crawling on the arterial wall at high-magnification. Images are presented as 2D extended depth-of-field pictures using maximum intensity projection. Green are myeloid cells, blue shows collagen-derived second harmonic generation in the tunica adventitia, grey represents autofluorescence of the extracelular matrix in the tunica media; and red is 150kDa TRITC-Dextran in the circulating blood, thus demarcating the lumen. Scale bar, 25 µm.
Online Movie XIII	Two-photon imaging of leukocytes crawling on the stabilized carotid artery of *Lysm*$^{egfp/egfp}$*ApoE*$^{-/-}$ mice. Images are presented as as 3D reconstructions. Movie shows cells isolated from the XYZT series in Sup. Mov. 12 by selecting the GFP emission channel which is subsequently projected in 3D using isosurface rendering. Scale bar, 25µm.